Material related effects on wet chemical micromachining of smart MEMS devices

A. Hein*[a], S. Finkbeiner[a], J. Marek[a], E. Obermeier[b]
[a]Robert Bosch GmbH,
Tuebinger Str. 123, D-72762 Reutlingen, Germany
[b]Technical University of Berlin, Department of Electrical Engineering, Germany

ABSTRACT

Smart MEMS devices such as pressure, mass flow and yaw rate sensors are presented in detail. One common point of this range of devices is their fabrication technology regarding anisotropic etching. This paper is first meant to give a short review upon the applications processed by using wet chemical etching in KOH-solutions. Furthermore, we will discuss about the impact of material and process related defects in the silicon crystal and on the anisotropic etching behavior.

Keywords: MEMS devices, bulk micromachining, crystal defects, metallic impurities, polishing

1. INTRODUCTION

With reducing size and increasing complexity of bulk micromachined devices such as pressure, mass flow and yaw rate sensors the wet chemical etching has become a key technology step for further yield increase. In this context the material quality seems to be a yield limiting factor in a production process using anisotropic etching. Any irregularity of the silicon material or in the process flow results in a considerable variation of the etching behavior. Adequate understanding of the various mechanisms taking place during high temperature process is crucial for successful fabrication of MEMS devices.

2. APPLICATIONS USING ANISOTROPIC ETCHING

2.1. Pressure Sensors

Figure 1 shows a schematical cross section of an integrated pressure sensor. A standard bipolar process is used for the manufacturing of the evaluation circuit on the front side of the wafer. During the bipolar process the piezo-resistors as well as the interconnects are manufactured for the sensing element. After the bipolar process the wafer is polished and exposed with the structure of the cavity on the backside. Anisotropic etching in KOH-solutions is used to obtain the cavity by means of an electrochemical etch stop.

The etching stops automatically at the interface of the buried layer which has been diffused in this area during the bipolar process. The silicon wafer is attached to a plate of pyrex glass by anodic bonding.

A pressure difference across the membrane results in a mechanical deflection of the plate. The resulting mechanical strain has a maximum in the middle of the edges of the membrane. Piezo-resistors have been diffused in this area during the bipolar process [1].

---

*Correspondence: Email: aylin.hein@de.bosch.de; Telephone: + 49 7121 35 1184; Fax: + 49 7121 35 4351

Part of the SPIE Conference on Micromached Devices and Components V
Santa Clara, California • September 1999
SPIE Vol. 3876 • 0277-786X/99/$10.00

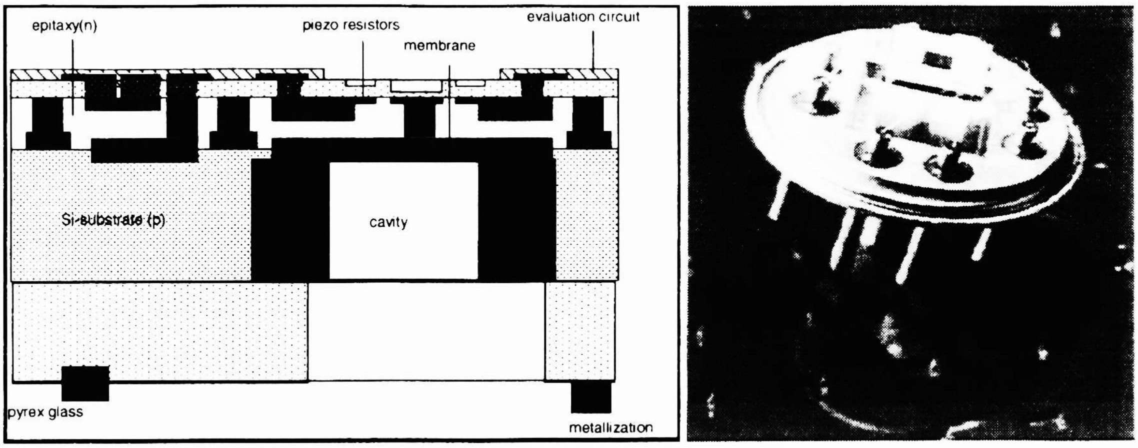

Fig. 1: *Cross section and the image of the integrated pressure sensor.*

2.2. Mass Flow Sensors

Figure 2 and *Figure 3* show a micromechanical air flow sensor. A thin dielectric membrane has been anisotropically etched in order to achieve a good thermal isolation of the sensing elements. In the middle of the membrane a heating element is deposited. A heating current increases the temperature in the middle of the membrane. Without air flow the thermal profile is symmetrical to both sides of the heating element. To the left and to the right of the heating element two temperature sensors are located. An air flow from the left side decreases the temperature on this side of the membrane; the temperature sensor T1 detects a lower temperature. The measurement of the difference between the left and the right temperature sensor is a direct indicator of the air flow over the chip.

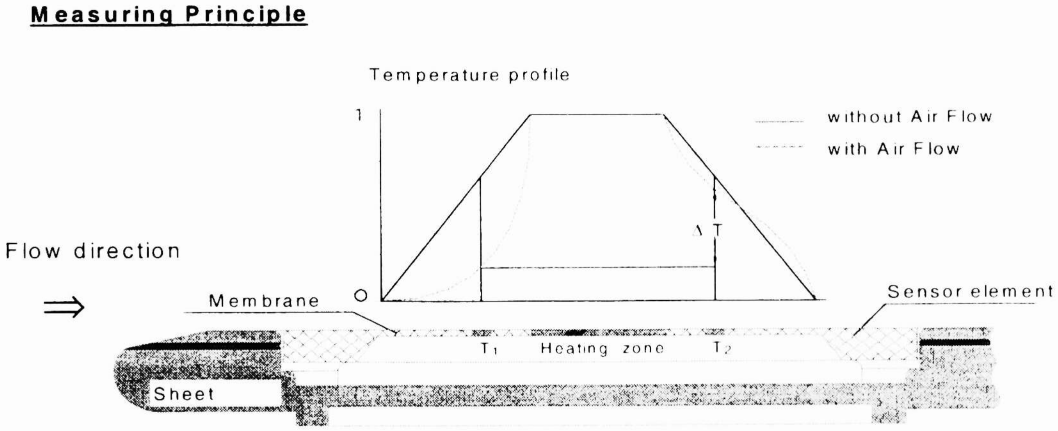

Evaluation of temperature difference $\Delta T = T_2 - T_1$

⇒ Characteristic curve dependent on flow direction

Fig. 2: *Measurement principle of the micromechanical mass flow sensor.*

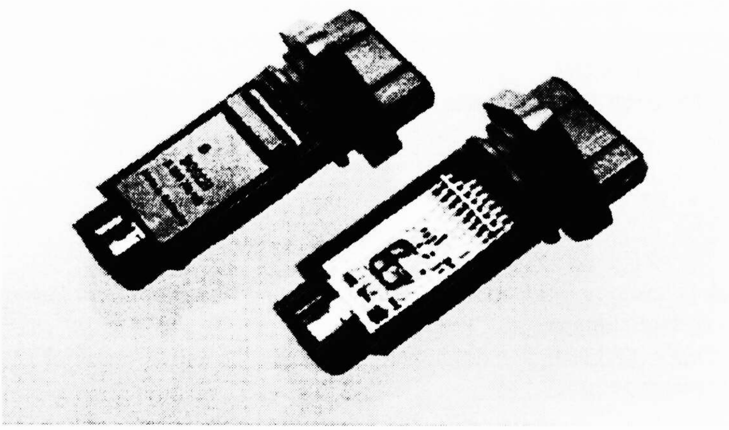

Fig. 3: *Image of the micromechanical mass flow sensor .*

2.3. Yaw Rate Sensors

A precision yaw rate sensor can be realized using a combination of surface and bulk micromachining (*Figure 4*): Two plates have been removed using anisotropic etching in KOH. Each of the plates is suspended by four folded beams at each of the edges. Aluminum wires are deposited on to these springs and plates. An oscillating electrical current in combination with a magnetic field drives the two plates at the resonant frequency. On top of the oscillating masses two acceleration sensors using surface micromachining have been manufactured. A rotation along the axis perpendicular to the wafer results in a Coriolis force in the wafer plane; the acceleration sensors are deflected from their center position. The difference between the acceleration sensors measures the yaw rate along the perpendicular axes.

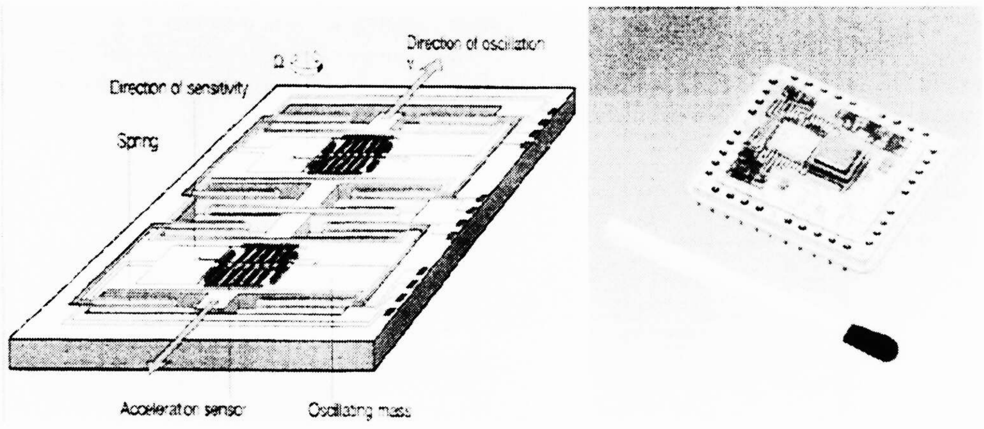

Fig. 4: *Principle of the yaw rate sensor (left), high precision yaw rate sensor using surface and bulk micromachining (right).*

All of these presented devices are processed by using anisotropic etching in KOH solutions. In the following we will discuss about some observations and developments in this key technology step.

3. WET CHEMICAL MICROMACHINING

KOH etching of silicon depends on many parameters, such as crystal orientation [2], dopant type and concentration [3], temperature, concentration and dissolved gases in KOH-solutions [4]-[5], surface stress effects [6], misalignment (mask, flat), etc. This list is by far not complete, yet there are still some dependencies to investigate.

Further etching results reveal three further kinds of yield limiting parameters of wet chemical etching: the bulk effects deriving from the initial oxygen content of the silicon (O_i), the surface effects generated by the presence of damage zone and finally dissolved metallic impurities in KOH.

In the following we will first focus on the heat treatment effects, especially regarding the initial oxygen concentration of silicon.

3.1. Bulk effects

The underetch rate of the mask is strongly influenced by the oxygen concentration in bipolar processed silicon: the lower the oxygen content, the lower the underetching rate.

Oxygen precipitates and the OSFs (Oxide-Induced-Stacking-Faults) in the initial material as can be seen in *Fig. 6* might generate the irregularity of the etching results.

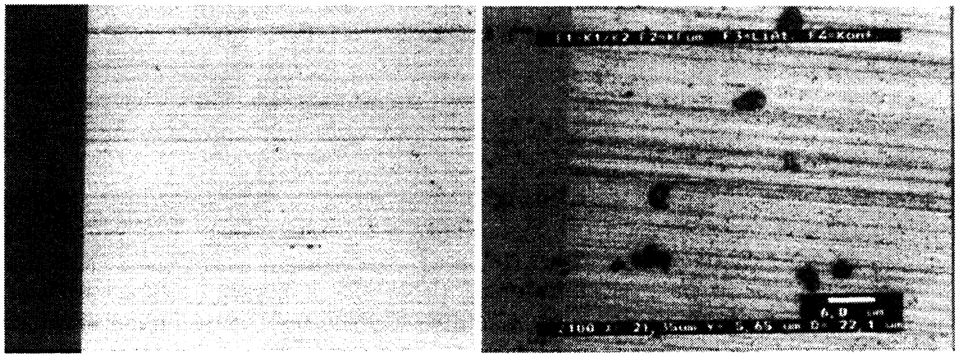

Fig. 5: Optical microscope images of bipolar processed bulk silicon after decoration in secco etch prior to etching in KOH with different interstitial oxygen content (left, 13.5 ppm; right, 15.5 ppm) [7].

The defect irregularities in the high temperature processed silicon initiates a change in the mask underetch rate which can clearly be seen in *Fig. 7.* shows the dependence of the mask underetching as a function of oxygen content: the underetching of the mask is constant within the range of 11 to 13 ppm. Between 13 and 14 ppm oxygen there is a transition point followed by a saturation at more than 15 ppm oxygen in silicon.

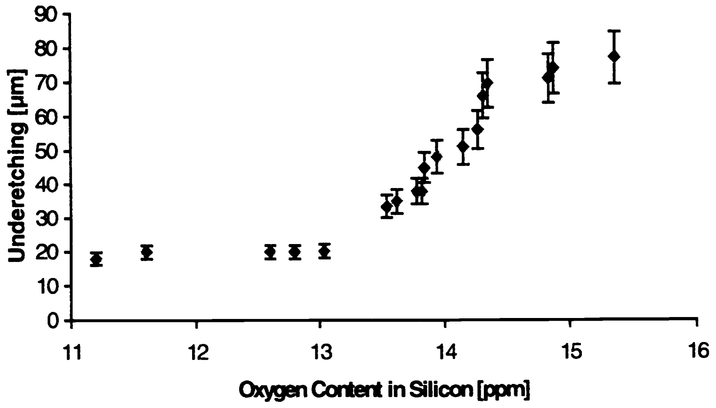

Fig. 6: Underetching of the mask versus oxygen content in the silicon substrate.

The behavior presented in *Fig. 6* can be explained by a simple physical model based upon the observation that for low O_i no precipitates and for high O_i a saturation of the precipitated oxygen density was found [7]-[8]. The transition region at around 14 ppm O_i is dominated by the increase of oxygen precipitate concentration.

A physical relation for the oxygen concentration and the underetching can be derived by fitting the etching results. The entire underetching UE_{entire} can be modeled as following in *Eq. 1*:

$$UE_{entire} = UE_0 + UE_{Oi} * (1 - e^{-\frac{[Oi]}{[x]}}) \qquad Eq.1$$

with
UE_0 = all non-oxygen related factors
UE_{Oi} = oxygen-dependent factors
$1 - e^{-\frac{[Oi]}{[x]}}$ = transition term

Fitting *Eq. 1* to the data points yields the unknown parameters (*Table 1*):

Table 1: Calculated Parameters of Eq. 1.

Parameter	**Value**
UE_0 [µm]	18,14
UE_{0i} [µm]	56,22
$[O_i]$ [ppm]	1,3e+014

After KOH-etching and decorating in secco-etch the crystal defects and the oxygen precipitates on the sidewalls of the cavity were examined. Surface roughness of the sidewalls ({111}-planes) is, as we could see qualitatively on Figure 7, strongly influenced by the oxygen content of the initial silicon as well. The most striking effect of oxygen seems to be the initiation of craters. This observation is in agreement as reported elsewhere [9].

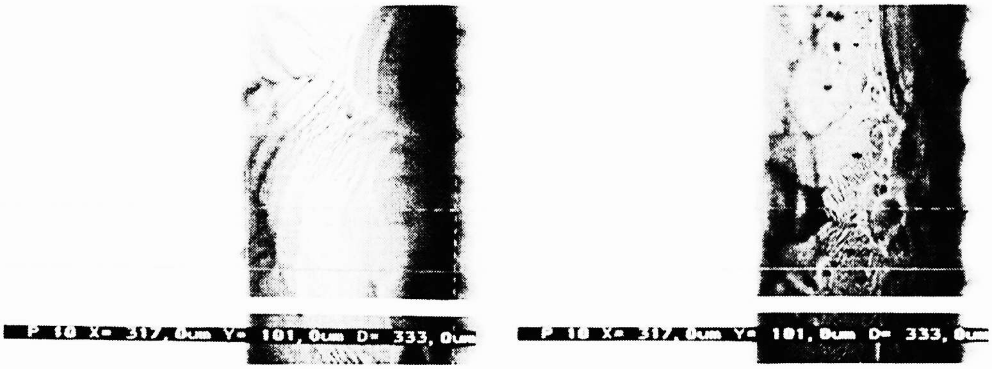

Fig. 7: Images of the surface topography of {111}-sidewalls with 30 µm underetching (left) and with 80 µm underetching (right).

3.1.1. Thermal Treatment

Some investigations on the stepwise thermal treatment of [100]-CZ- and FZ-silicon reveal interesting changes on the crystal defects and the etching behavior in KOH. The anisotropy (the quotient of the vertical etch rate and the underetching of the mask), formed crystal defects as well as the surface roughness of the exposed {100}- and {111}-planes are visibly affected by high temperatures (T>1000°C).

As thermal treatment of the silicon substrate can result in a precipitation of the interstitial oxygen, the precipitated part of oxygen causes elastic stress in the crystal which can be relieved by an generation of defects. We found out that evolution of these defects accelerates the lateral etch rate considerably. For the reference, the samples without thermal treatment the anisotropy have a value of 120 for FZ-silicon and 70 for CZ-silicon, respectively. However, with rising temperature and process time the anisotropy decreases to 30 for FZ-silicon and 15 for CZ-silicon (Figure 8).

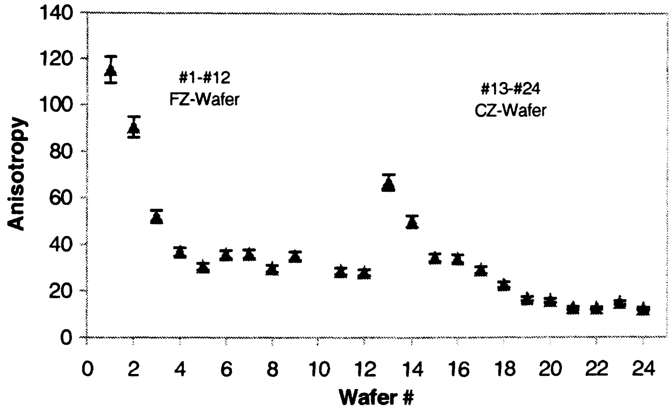

Fig. 8: Dependence of the anisotropy on the high temperature process steps.

3.2. Surface parameters

The wet chemical etching behavior can be affected by surface parameters just as the stress and the so-called damage zone. The last parameter is induced by a grinding step, followed by the polishing step of the substrate. The thickness of the damage zone is given in the literature as few microns to some ten microns.

Following discussions deal with the experiments regarding the damage zone as the impact of the passivation stress on the etching behavior found out to be negligible.

To find out the influence on the thickness of the damage zone we polished the half of the lot after standard grinding process 10 µm and the other half 20 µm. The following picture demonstrates the observed dependence of the underetching on the polishing depth.

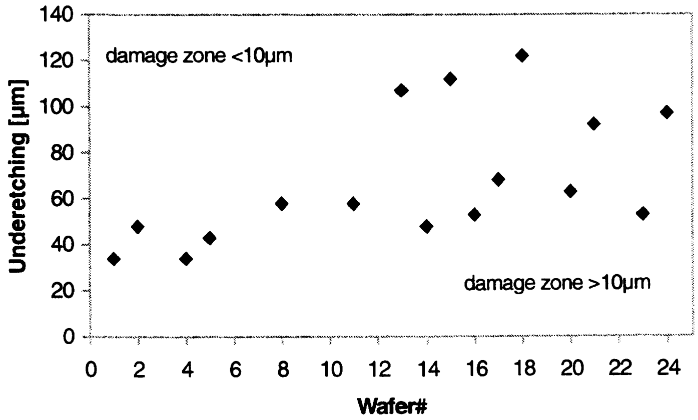

Fig. 9: Underetching of the mask versus thickness of the damage zone.

The significant result which can be deduced from Figure 9 is that the underetching has relatively low values when polished deeper corresponding to a small thickness of the damage zone. A standard polishing might initiate in some cases a low grade of the underetching as well, however as observed at wafer # 13, 15, 18, etc. a high degree of variation.

All of these discussed factors as oxygen content or the damage zone effect can more or less be referred to the technology steps of the presented devices. Pressure sensors, mass flow sensors or the yaw rate sensors show the same KOH etching behavior. But since they have different high thermal budgets, mass flow sensors, for instance, are less affected by the oxygen content of the initial silicon.

3.2. Impurities in the etchant

Another main influence to affect the etching behavior is the purity of the solution. This impact was investigated in purified KOH solutions containing metallic salts as shown in Figure 10. The anisotropy (the quotient of the vertical etch rate and the underetching of the mask), of silicon in aqueous solutions shows a significant dependence on the manufacturer of the etch chemicals and the production process, respectively. Ignoring this effect will have detrimental consequences on the success of the fabrication of precise devices.

The anisotropy is strongly affected by any chosen metallic impurity. Metals such as iron, sodium, chromium, aluminum and zinc result in an increase, while copper and nickel show a decrease of the anisotropy (Figure 10).

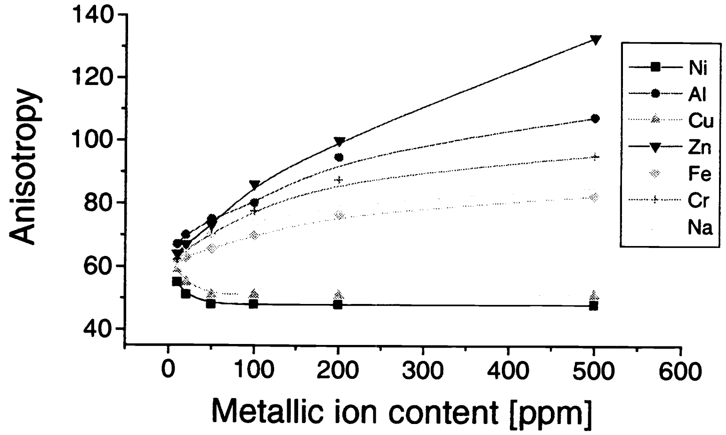

Fig. 10: Anisotropy versus metallic ion content in the KOH etching solution [4].

Another visible effect of the metallic impurities is the variation of the convex corners. The etching of rectangular convex corners in KOH solutions leads to a deformation of the edges due to corner undercutting. At lower metal ion content the angle has a value corresponding to {411} planes. However with increasing content the value of the angle approaches to the one of {311} planes (Figure 11).

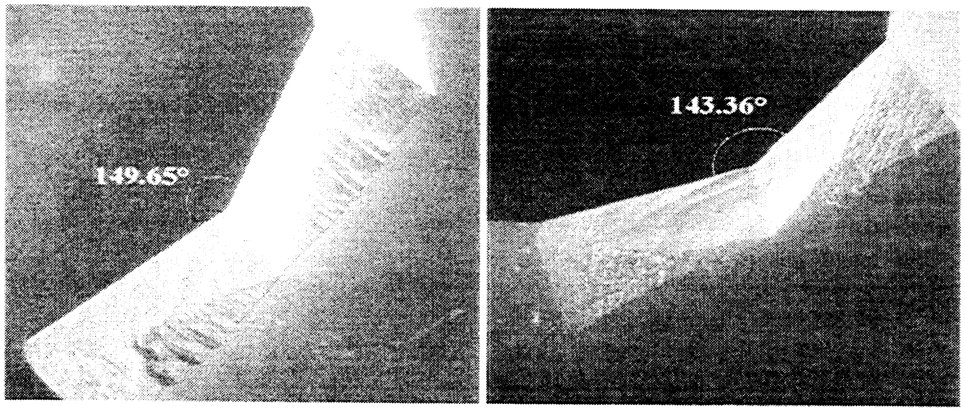

Fig. 11: SEM image of a convex corner etched without metal ion contamination (left) etched with copper content of 500 ppm (right).

4. CONCLUSION

In this paper the wet chemical etching behavior of smart MEMS devices such as pressure, mass flow and yaw rate sensors are presented and discussed.

Our results show main yield limiting factors in fabricating the micro devices: the bulk effects (oxygen content in silicon), the surface effects (damage zone initiated by grinding) and environmental effects (etchant purity) .

The impact of oxygen-related defects in silicon on the etching behavior are examined. Variations of the oxygen concentration in the substrate within the range from 11 to 16 ppm affect the etching behavior of silicon dramatically. The interstitial amount of oxygen has considerable impact on the underetching of the etching mask. The presence of oxygen precipitates has a detrimental effect on the underetching by producing unstable centers in the crystal during etching. Furthermore, we found that precipitated oxygen induces crystal defects such as stacking faults which possibly result in a mechanical stress in the silicon. This additional stress in the lattice might cause the observed higher degree of underetching.

Other noticeable parameters might be carbon and metallic impurities in the crystal. Their effect on the etching behavior is not yet very well investigated. It is to investigate how much the variation of the underetching and the surface roughness depends on non-oxygen related impurities such as carbon or copper and iron in silicon. For instance carbon is expected to enhance oxygen precipitation by acting as heterogeneous nucleus [10].

We observed that deep defects in the crystal induced by the grinding step are not removed by a standard polishing . A deeper polish of the silicon substrate results in a lower degree of underetching. Here we obtained 40 µm for the underetch rate with a small amount of variation. Polishing the wafer only 10 µm seems still to contain some rest of the damage zone initiating a variation of the underetching within a range of 40 to 120 µm.

Metallic ions in the etching solution within the range from 0 to 200 ppm affect the etching behavior of silicon dramatically. Beyond this value a saturation effect is observed. Metals such as iron, sodium, chromium, aluminum and zinc result in an increase, while copper and nickel decrease the anisotropy. The changes in the surface potential of silicon might be responsible for this observation. The presence of metal ions in the etching solution initiates higher surface roughness values as well. This might be the result of the adsorption of the metal ions on the silicon surface during the etching process. Furthermore, the dissolution of certain metals such as aluminum, zinc or sodium may also have a detrimental effect on the surface finish by producing more hydrogen bubbles when dissolving in the etching solution. Another effect of the metallic impurities is the variation of the convex corners. At lower metal ion content the angle has a value corresponding to {411} planes. However with increasing content the value of the angle approaches to the one of {311} planes.

This review is meant to give the reader a brief impression of several devices processed by using bulk micromachining and some observations made during the etching step. It is of course by no means complete, to help the reader to find more information a few key references are provided.

REFERENCES

[1] J. Marek " *Microsystems in Automotive Applications*" MST 1998 Potsdam, 43 (1998)

[2] P. H. Hesketh et al. "*High index plane selectivity in silicon anisotropic etching in aqueous potassium hydroxide and cesium hydroxide*" Thin Solid Films, 215, 58 (1992)

[3] H. Seidel et al. *"Anisotropic Etching of Crystalline Silicon in Alkaline Solutions"* J. Electrochem. Soc., Vol. 137, No 11, 3626 (1990)

[4] A. Hein, O. Dorsch, E. Obermeier "*Effects of metallic impurities on anisotropic etching of silicon in aqueous KOH-solutions",* Transducers 97, Chicago, USA (1997)

[5] S. A. Campbell "*Inhibition of pyramid formation in the etching of Si p<100> in aqueous potassium hydroxide-isopropanol*" J. Micromech. Microeng. 5 (1995) 209-218.

[6] H. Seidel et al., J. Electrochem. Soc., Vol. 137, No 11, 3612 (1990)

[7] A. Hein, S. Finkbeiner et al. "*The Effects of Impurities in Silicon on Anisotropic Etching in KOH-Solutions*", MST 98, Postdam, Germany (1998)

[8] A. Hein, S. Finkbeiner et al. *"The Effects of Thermal Treatment of CZ-and FZ-Silicon on Crystal Defect Formation and the Etching Behavior during Anisotropic Etching in KOH-Solutions",* Transducers 99, Sendai, Japan (1999)

[9] C. Merveille "*Surface quality of {111} side-walls in KOH-etched cavities*" Sensors and Actuators A, 60, 244 (1997)

[10] W. Wijaranakula, J. Matlock "*A formation of crystal defects in carbon-doped Czochralski-grown silicon after a three-step internal gettering anneal"* J. Electrochem. Soc. 138 (1991) 2153.